We are IntechOpen, the world's leading publisher of Open Access books Built by scientists, for scientists

6,900
Open access books available

186,000
International authors and editors

200M
Downloads

Our authors are among the

154
Countries delivered to

TOP 1%
most cited scientists

12.2%
Contributors from top 500 universities

WEB OF SCIENCE™

Selection of our books indexed in the Book Citation Index in Web of Science™ Core Collection (BKCI)

Interested in publishing with us?
Contact book.department@intechopen.com

Numbers displayed above are based on latest data collected.
For more information visit www.intechopen.com

2

New Infrared Luminescence from Bi-doped Glasses

Yasushi Fujimoto
Institute of Laser engineering, Osaka University
Japan

1. Introduction

Infrared luminescent materials are widely used as laser media, for example, Nd:YAG and Er-doped silica fibers. In the infrared region, luminescence offers many advantages as laser media due to the variety of optics and excitation sources, such as semiconductor lasers and flash lamps. A frequency-doubled laser-beam with a nonlinear crystal can also obtained in the visible region. Therefore, infrared light source materials are very useful for scientific research and industrial uses.

Fujimoto et al. discovered a new infrared luminescent from bismuth-doped silica glass (BiSG)(Fujimoto & Nakatsuka 2001). Wide luminescent exists between 1000 and 1600 nm, and absorption is in the visible region. The lifetime is 630 μs at room temperature. Since this silica glass-based material has luminescence around 1.3 μm of zero-dispersion wavelength, it can be used as a core material of an optical fiber amplifier for telecommunication in the 1.3-μm range. Fujimoto et al. also demonstrated an optical amplification at 1.3 μm with 0.8-μm excitation(Fujimoto & Nakatsuka 2003). Therefore, BiSG is expected to be a promising substitution for Pr^{3+}:ZBLAN fiber or Raman amplifiers in the 1.3-μm region.

The spectroscopic properties of BiSG are different from previously reported Bi luminescent material(Fujimoto & Nakatsuka 2001), because the previous Bi-doped glasses or crystals with low Bi_2O_3 concentration showed that luminescences exist in the visible region (400 ~ 600 nm) and that absorptions are in the ultraviolet region. The lifetimes (~4 μs) are much shorter than those of BiSG at room temperature. Such luminescences have been reported to originate from the Bi^{3+} ion in the media(M. J. Weber & Monchamp 1973; Parke & Webb 1973; van der Steen, van Hesteren et al. 1981). BiSG is also different from the Bi_2O_3-rich glass whose Bi_2O_3 concentration ranges from 18.7 to 42.5 mol%(Sugimoto, Kanbara et al. 1996) because the glass has no absorption in the visible region. Then the investigation of new glass compositions with Bi luminescence is also progressing vigorously in a past decade. Although the first discovered glass was a silica-based material with a SiO_2 of 97.5 mol%(Fujimoto & Nakatsuka 2001), many glass compositions were tested and shown to effectively generate Bi luminescence, such as silicate(Peng, Qiu et al. 2005; Ren, Yang et al. 2006; Suzuki & Ohishi 2006; Arai, Suzuki et al. 2007; Murata & Mouri 2007; Peng, Chen et al. 2007; Ren, Qiu et al. 2007; Zhou, Feng et al. 2007; Peng, Wu et al. 2008), germanate(Peng, Qiu et al. 2004; Meng, Qiu et al. 2005; Peng, Meng et al. 2005; Peng, Qiu et al. 2005; Peng, Wang et al. 2005; Wang & Xia 2006; Xia & Wang 2006; Murata & Mouri 2007; Ren, Wu et al. 2007;

Source: Advances in Solid-State Lasers: Development and Applications, Book edited by: Mikhail Grishin,
ISBN 978-953-7619-80-0, pp. 630, February 2010, INTECH, Croatia, downloaded from SCIYO.COM

Ren, Dong et al. 2007; Ren, Qiao et al. 2007; Ren, Qiu et al. 2007; Ren, Qiu et al. 2007; Peng, Wu et al. 2008; Qiu, Peng et al. 2008), borate(Meng, Qiu et al. 2005; Murata & Mouri 2007; Qiu, Peng et al. 2008), germanosilicate(Ren, Dong et al. 2007; Ren, Dong et al. 2008), and phosphate(Meng, Qiu et al. 2005; Qiu, Peng et al. 2008) glasses.
In this chapter, the author will introduce the basic properties of Bi doped silica glass (BiSG), such as a phase diagram and spectroscopic properties, and then mainly talk about the origine of luminescent center.

2. Basic properties of BiSG

2.1 Phase diagram

A phase diagram of BiSG was obtained for the Bi_2O_3-Al_2O_3-SiO_2 glass system. Silica powder (Aerosil 50; SiO_2, 99.8%), bismuth-oxide (Kojundo Chemical Lab. Co., Ltd.; α-Bi_2O_3, 99.99%), and aluminum oxide (Kojundo Chemical Lab. Co., Ltd.; α-Al_2O_3, 99.99%) were used as reagents. A properly mixed powder was inserted into a silica tube with an inner/outer diameter of 1/3 mmϕ, and then the tube was heated by a mixed gas burner of natural gas and oxygen. After heating, the powder was checked for a distinctive glassy wetting. If it had such wetting, the composition was determined to be the glassy phase in the Bi_2O_3-Al_2O_3-SiO_2 glass system.
The measured phase diagram of the Bi_2O_3-Al_2O_3-SiO_2 glass system is shown in Fig. 1. The circle, triangle, and cross points show the glassy wetting states (pink to reddish-brown), unclear glassy states (pink to reddish-brown), and no glassy state (reddish-brown), respectively. This phase diagram shows a tendency where the glass whose Al_2O_3 content is larger than Bi_2O_3 is well glassified above a 90% SiO_2 concentration. On the other hand, all the samples are glassified at a 80% SiO_2 concentration without dependence on the Bi_2O_3 or Al_2O_3 content. The infrared luminescent spectrum is observed until 10 mol% of Bi_2O_3 concentration.

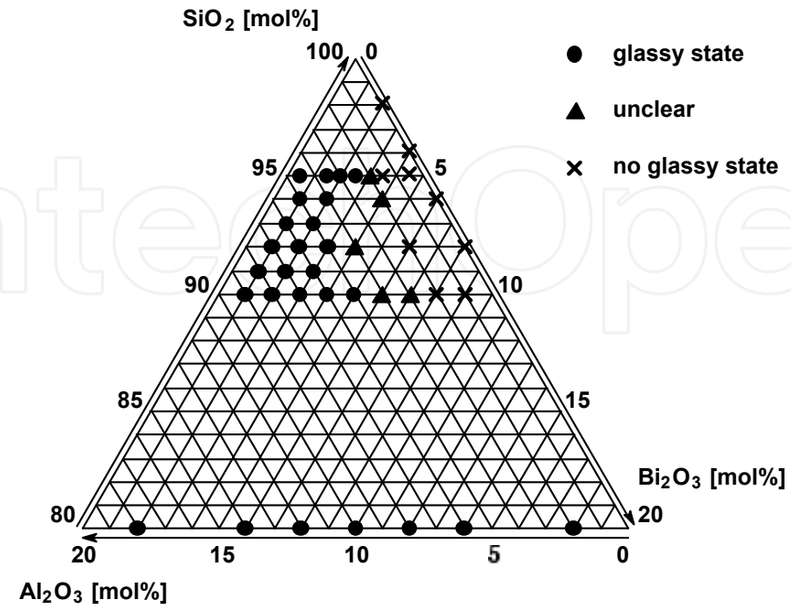

Fig. 1. Measured phase diagram of Bi_2O_3-Al_2O_3-SiO_2 system.

2.2 Influence of additives on luminescent intensitys

The Bi_2O_3-Al_2O_3-SiO_2 glass system is affected by alkaline metal additive. Figure 2 shows an effect of Li_2O additive in BiSG. The glass composition is Bi_2O_3(1.0 mol%)-Al_2O_3(7.0 mol%)-SiO_2(92-x mol%)-Li_2O(x mol%) glass system. The luminescent intensity decreases with increasing Li_2O additive drastically (Seo, Fujimoto et al. 2006). Therefore, in order to get luminescent center, we should carefully choose the host composition.

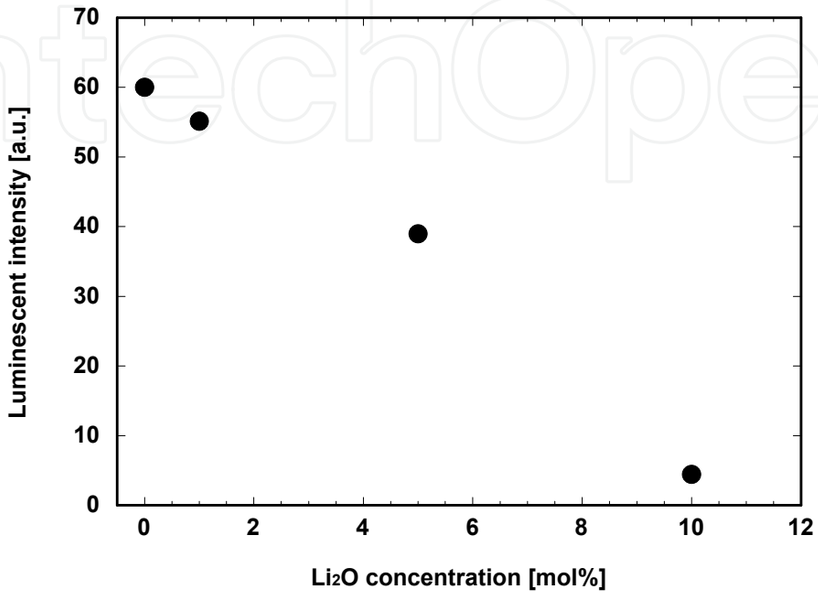

Fig. 2. Luminescent intensity dependence on Li_2O concentration for Bi_2O_3(1.0 mol%)-Al_2O_3(7.0 mol%)-SiO_2(92-x mol%)-Li_2O(x mol%) glass system.

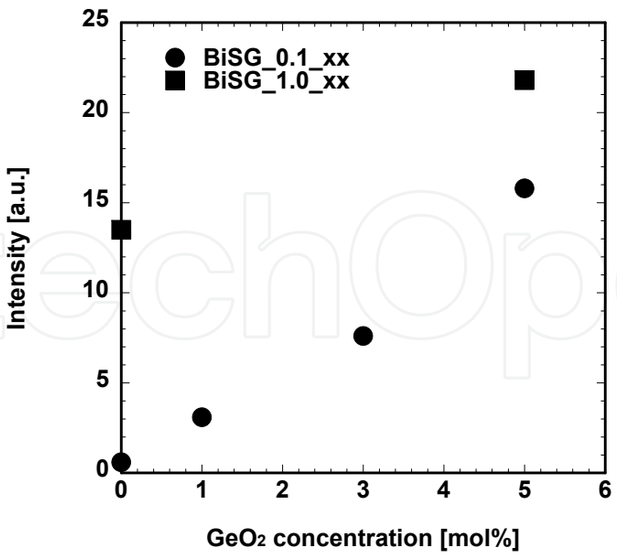

Fig. 3. Dependence of lumienscent intensity on GeO_2 additive. The filled circle denotes BiSG with 0.1 mol% Bi_2O_3 concentration, while the filled square represents that of 1.0 mol% Bi_2O_3 concentration. The nomenclature of the samples is as follows: for example, the sample name "BiSG_1.0_5.0" means that the composition is Bi_2O_3 = 1.0 mol%, GeO_2 = 5.0 mol%.

On the other hand, GeO_2 is the one of attractive additive to increase luminescent intensity of BiSG (Fujimoto, Hirata et al. 2007). Figure 3 shows the dependence of luminescent intensity on GeO_2 concentration. All the samples contain 7.0 mol% of Al2O3. The nomenclature of the samples is as follows: for example, the sample name "BiSG_1.0_5.0" means that the composition is Bi_2O_3 = 1.0 mol%, GeO_2 = 5.0 mol%. The luminescent intensity of BiSG grows with increasing GeO_2 concentration almost linearly for BiSG_0.1_xx samples, and the luminescent intensity of BiSG_0.1_5.0 is 26.3 times larger than that of BiSG_0.1_0.0 only because of the GeO_2 additive. The increment effect on BiSG with GeO_2 additive is also observed for a Bi_2O_3 concentration of 1.0 mol% (BiSG_1.0_5.0), but it is less remarkable than for the lower Bi_2O_3 concentration of 0.1 mol%. Furthermore, the increment is only about 1.5 times larger than for BiSG without GeO_2 (BiSG_1.0_0.0). On the other hand, the luminescent intensity of BiSG_0.1_5.0 is almost same as that of BiSG_1.0_0.0. According to these data, the GeO_2 additive effectively increases the luminescent intensity of BiSG, and this effect is especially remarkable at low Bi_2O_3 concentrations.

2.3 Spectroscopic properties

The typical spectroscopic properties of BiSG are shown in Fig. 4. Five main absorption bands exist between 250 and 2000 nm: 300 (A), 500 (B), 700 (C), 800 (D), and 1000 nm (E) (Fig. 5(a)). It is considered that absorption band A is mainly derived from O^{2-} in the base glass(Scholze 1991). The other four absorptions (B~E) are connected to the infrared emissions shown in Fig. 5(b). Each luminescent peak wavelength and full width at half maximum (FWHM) were recognized as 1182 and 300 nm at 500-nm excitation, 1144 and 192 nm at 700 nm, 1265 and 336 nm at 800 nm, and 1130 and 188 nm at 1000 nm. A similarity of the luminescent spectra can be seen between 700- and 1000-nm excitations. These spectroscopic properties are different from the Bi^{3+} ones(M. J. Weber & Monchamp 1973; Parke & Webb 1973; van der Steen, van Hesteren et al. 1981)(Table 1).

	Bi^{3+}:Glass*1 ($Na_2O \bullet P_2O_5$)	Bi^{3+}:Crystal*2 ($Bi_3Ge_4O_{12}$)	BiSG *3
Excitation wavelength [nm]	250	290	500~800
Luminescent wavelength [nm]	390	480	1000~1400
Lifetime [μs] (room temp.)	3.9	0.1	630

*1 (Parke & Webb 1973), *2 (M. J. Weber & Monchamp 1973), *3 (Fujimoto & Nakatsuka 2001)

Table 1. Differences of spectroscopic properties between BiSG and previously reported Bi^{3+} luminescent material.

3. The origin of luminescent center

After the discovery of a new infrared luminescent bismuth center, several research groups try to understand what is the origine of the luminescence. Although there have been many previous discussions on this distinctive luminescent center, it has remained unclear. Different authors tentatively assigned the different origins of this near infrared luminescence to the electronic transition derived from Bi^{5+}(Fujimoto & Nakatsuka 2001; Dvoyrin, Mashinsky et al. 2006; Fujimoto & Nakatsuka 2006; Wang & Xia 2006; Xia & Wang 2006; Ohkura, Fujimoto et al. 2007), Bi^{2+}(Ren, Qiu et al. 2007; Ren, Qiu et al. 2007; Ren, Qiu et al. 2007; Ren, Dong et al. 2008), and Bi^{+}(Meng, Qiu et al. 2005; Meng, Qiu et al. 2005;

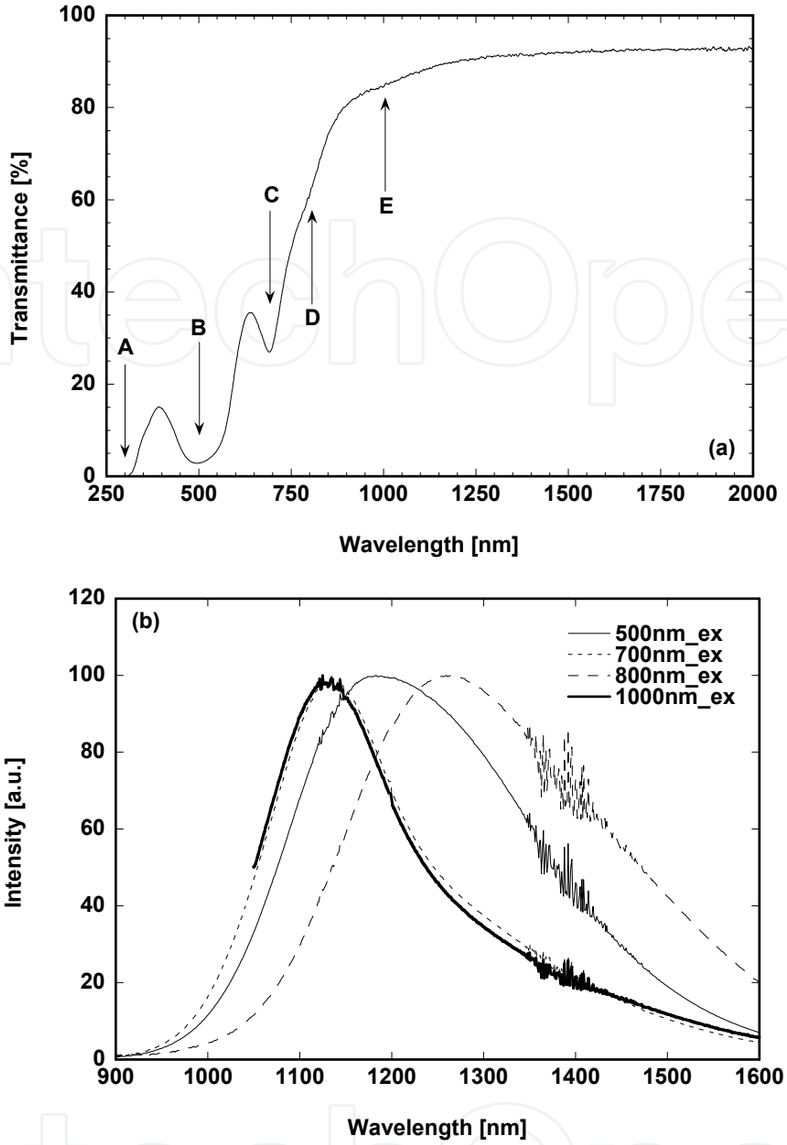

Fig. 4. Typical spectroscopic properties of BiSG (sample B1 in Table 2): (a) transmittance spectrum shows five main absorption bands between 250 and 2000 nm, including 300 nm (A), 500 nm (B), 700 nm (C), 800 nm (D), and 1000 nm (E), and (b) luminescent spectra excited by 500, 700, 800, and 1000 nm.

Dvoyrin, Mashinsky et al. 2006; Arai, Suzuki et al. 2007; Ren, Qiu et al. 2007; Ren, Qiu et al. 2007; Ren, Qiu et al. 2007; Yang, Chen et al. 2007; Zhou, Feng et al. 2007; Qiu, Peng et al. 2008; Ren, Dong et al. 2008; Truong, Bigot et al. 2008) or to that of BiO molecules(Ren, Yang et al. 2006; Murata & Mouri 2007; Peng, Chen et al. 2007; Peng, Wu et al. 2008) dispersed in the glass host. Since most of these proposals were however analogized from only spectroscopic mesurement analysis, uncertainty remains in the present discussions. In addition, even the same researchers offer several explanations, suggesting that spectroscpic analogy is insufficient to correctly understand the luminescent center or the luminescent mechanism.

Based on this viewpoint, our group discarded the spectroscopic analogical approach to understand the structure of the luminescent center or its mechanism and instead chose such instrumental analytical approaches as nuclear magnetic resonance (NMR), x-ray diffraction (XRD), electron spin resonance (ESR), x-ray photoelectron spectroscopy (XPS), and extended x-ray absorption fine structure (EXAFS). NMR data revealed the coordination structure of the specific ions in a material, ESR and XPS data provided the valence state of ions, and EXAFS offered the bonding distance between the specific and neighboring ions. Once these analytic instrumental data are integrated to build one possible figure of a luminescent center, then the luminescent mechanism will be discussed, because knowledge of the luminescent center is very useful for understanding the luminescent mechanism, which is obviously important for such optical applications as lasers or amplifiers.
In the following paragraphs, let's try to build up an image of the local structure of the Bi luminescent center based on the analytical data, such as, spectroscopic properties (SPCT), luminesent intensity (LMI), NMR, XRD, ESR, XPS, and the EXAFS data of BiSG in a simple Bi_2O_3-Al_2O_3-SiO_2 glass system without discrepancies. From this approach, we will reach one strongly possible local structure of a distinctive Bi luminescent center that consists of Bi and Al that exist closely to each other.

3.1 Sample preparation

In these analyses, composition of BiSG is very important, because Bi infrared luminescent center, as shown in section 2.2, is disappeared with increasing some additives in the host. This means that majority part of Bi ions in the host shifts to non-emissive site, thus even if we choose the multi-component glass system and analyze the Bi centers, we could not judge the results form an inherent luminescent center or the other non-emissive site, then we would go into the complicated maze. Therefore, the analyses should be carried out to concentrate on the simple three components system, Bi_2O_3-Al_2O_3-SiO_2 glass system.
The samples for the instrumental analyses were prepared as follows.

1. A-series: The ratio of Bi_2O_3 to Al_2O_3 was kept at 3/7, and the Bi_2O_3 concentration varied from 0.1, 0.3, 0.5, 1.0, and 3.0 mol%. These samples were called A1-A5, respectively. Their compositions are inside the glassy phase area in Fig. 1.
2. B-series: B1 was composed of Bi_2O_3 (1.0 mol%), Al_2O_3 (7.0 mol%), and SiO_2 (92.0 mol%). This was used for the measurement of the spectroscopic properties because Al_2O_3-rich BiSG includes few bubbles. B2 was composed of Bi_2O_3 (0.3 mol%), Al_2O_3 (2.3 mol%), and SiO_2 (97.4 mol%) and B3 of Bi_2O_3 (3.0 mol%), Al_2O_3 (7.0 mol%), and SiO_2 (90.0 mol%). They were used for the ESR measurements.
3. C-series: C1 was composed of Bi_2O_3 (1.0 mol%) and SiO_2 (99.0 mol%) without Al_2O_3, and C2 was composed of Al_2O_3 (2.3 mol%) and SiO_2 (97.7 mol%) without Bi_2O_3. C1 and C2 were dark brown and colorless, respectively. C1 had no glassy wetting, but C2 did.

The chemical composition of the investigated BiSG samples and the several standards are listed in Table 2. Silica powder (Aerosil 50; SiO_2, 99.8%), bismuth-oxide (Kojundo Chemical Lab. Co., Ltd.; α-Bi_2O_3, 99.99%), and aluminum oxide (Kojundo Chemical Lab. Co., Ltd.; α-Al_2O_3, 99.99%) were used as reagents to make the glass samples of the Bi_2O_3-Al_2O_3-SiO_2 glass system. The mixtures of these powders were melted in an aluminum crucible in an electric furnace at 1750°C in air, and the melts were annealed by natural cooling. All of these glasses were reddish-brown. $NaBiO_3$ (Kanto Chemical Co., Inc.; >80%), which was identified as $NaBiO_3 \cdot 2H_2O$ by XRD(PDF#30-1161 2000), α-Bi_2O_3, and Bi-metal (Kojundo Chemical Lab. Co., Ltd.; 99.9%) were used as standard materials for the analyses.

Sample	Bi_2O_3[mol%]	Al_2O_3[mol%]	SiO_2[mol%]	Measurements
<BiSG>				
A1	0.1	0.23	99.67	LMI, NMR, XRD
A2	0.3	0.7	99.0	LMI, NMR, XRD, EXAFS
A3	0.5	1.15	98.35	LMI, NMR, XRD, EXAFS
A4	1.0	2.3	96.7	LMI, NMR, XRD, EXAFS, XPS
A5, B3	3.0	7.0	90.0	LMI, NMR, ESR, XRD, EXAFS, XPS
B1	1.0	7.0	92.0	SPCT
B2	0.3	2.3	97.4	ESR
C1	1.0	0.0	99.0	LMI
C2	0.0	2.3	97.7	NMR, XRD
<Aluminium standard>				
α- Al_2O_3	0.0	100	0.0	NMR, XRD
<Bismuth standards>				
$NaBiO_3$	---	---	---	EXAFS, XPS
α- Bi_2O_3	100	0.0	0.0	EXAFS, XPS
Bi metal	---	---	---	EXAFS, XPS

LMI: Luminescent Intensity, NMR: ^{27}Al-NMR(Nuclear Magnetic Resonance), XRD: X-ray Diffraction, ESR: Electron Spin Resonance, XPS: X-ray Photoelectron Spectroscopy, EXAFS: Extended X-ray Absorption Fine Structure, SPCT: Spectroscopic Properties

Table 2. List of chemical composition and performed measurements for investigated Bi doped silica glasses and Al, Bi standards.

The prepared samples were evaluated by instrumental analyses, including spectroscopic measurements, NMR, XRD, ESR, XPS, and EXAFS. Luminescent intensity and spectra were measured by a spectrophotometer (JASCO Corporation; SS-25). Transmission spectra were obtained by a spectrophotometer (HITACHI; U-4100). The aluminum coordination state (ACS) in BiSG was determined by the ^{27}Al-NMR spectrum, and the ^{27}Al-NMR spectra were obtained on a nuclear magnetic resonance spectrometer (JEOL Ltd.; JNM-GSX-400). The XRD patterns were measured by an X-ray diffractometer (RIGAKU; RINT2500). The ESR signals were measured by an electron spin resonance spectrometer (JEOL Ltd.; JES-ME-2X) at both room and liquid nitrogen temperatures.

The XPS spectra were recorded on a SHIMADZU (KRATOS) AXIS 165 using Mg*K* radiation (1253.6 eV) with a beam size of 0.7 x 0.3 mm^2 and 50 eV analyzer pass energy. The operating vacuum pressure was maintained from 10^{-8} to 10^{-9} Torr. An electron beam was used to reduce the electrical charging during the measurements. Any binding energy shifts due to electrical charging were corrected by the C1*s* (284.6 eV) peak as an internal reference. 3-minute Ar-sputtering was used to remove the oxidized surface on the Bi-metal powder.

The Bismuth L_{III} XAFS spectra were measured in the transmission mode using a BL-7C beam line at the Photon Factory (PF). The ring energy was 2.5 GeV. The x-ray was monochromized by a Si(111) double crystal monochrometer. Two ionization chambers were used as detectors. A 170-mm length chamber was filled with Ar/N_2 (15%:85%) gas for

incident x-ray energy (I_0), and the other was 310-mm long with Ar-100% gas for transmitted x-ray energy (I). The EXAFS data of the Bi L_{III} edge (13426.5 eV) were collected between 12926 and 14526 eV with 481 energy points. Data analysis was carried out on *UWXAFS*. The back-scattering amplitude and the phase shift were theoretically calculated using *FEFF 8.2* code. The Debye-Waller factor was estimated by the Debye code implemented in *FEFF 8.2* based on Raman spectroscopy results(Narang, Patel et al. 1994).

3.3 Luminescent intensity

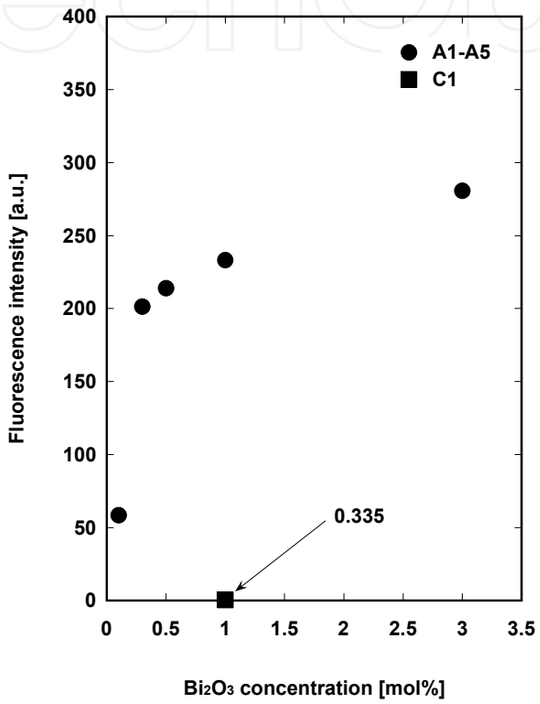

Fig. 5. Dependence of luminescent intensity (LMI) on Bi_2O_3 concentration detected at 1120-nm luminescence with 500-nm excitation.

The dependence of luminescent intensity (LMI) on Bi_2O_3 concentration is illustrated in Fig. 5. The measured samples were A-series (A1~A5) and C1. The excitation and detection wavelengths of the luminescence were at 500 and 1120 nm, respectively. The luminescent intensity nonlinearly increased with increased Bi_2O_3 concentration. At a 1.0 mol% of Bi_2O_3 concentration, the luminescent intensity from A4, which includes 2.3 mol% of Al_2O_3, is three orders of magnitude larger than that of C1 without Al_2O_3. Based on these results, we conclude the following:

1. Al_2O_3 additive can remarkably increase to generate a Bi luminescent center.
2. The generation of a Bi luminescent center has a nonlinear relation for Bi_2O_3 concentration.

3.4 ^{27}Al-NMR spectra

^{27}The Al-NMR spectra in BiSG are shown in Fig. 6(Fujimoto & Nakatsuka 2006). ^{27}Al chemical shifts were measured relative to $Al(H_2O)_6^{3+}$. The measured samples were A-series,

C2, and α-Al_2O_3. α-Al_2O_3 with a 6-fold coordinated state of corundum structure was used as a standard sample, and a peak exists at 15 ppm. The peaks at 70 and –40 ppm (marked by asterisks) were derived from spinning sidebands. The peaks of ^{27}Al-NMR from A1 to A3 only exist at 15 ppm and are the same as α-Al_2O_3. The A4 peak is still dominated by the 15 ppm peak, but a peak around 50 ppm begins to emerge, and then a peak of 56.4 ppm becomes dominant in A5 (Fig. 6(b)).

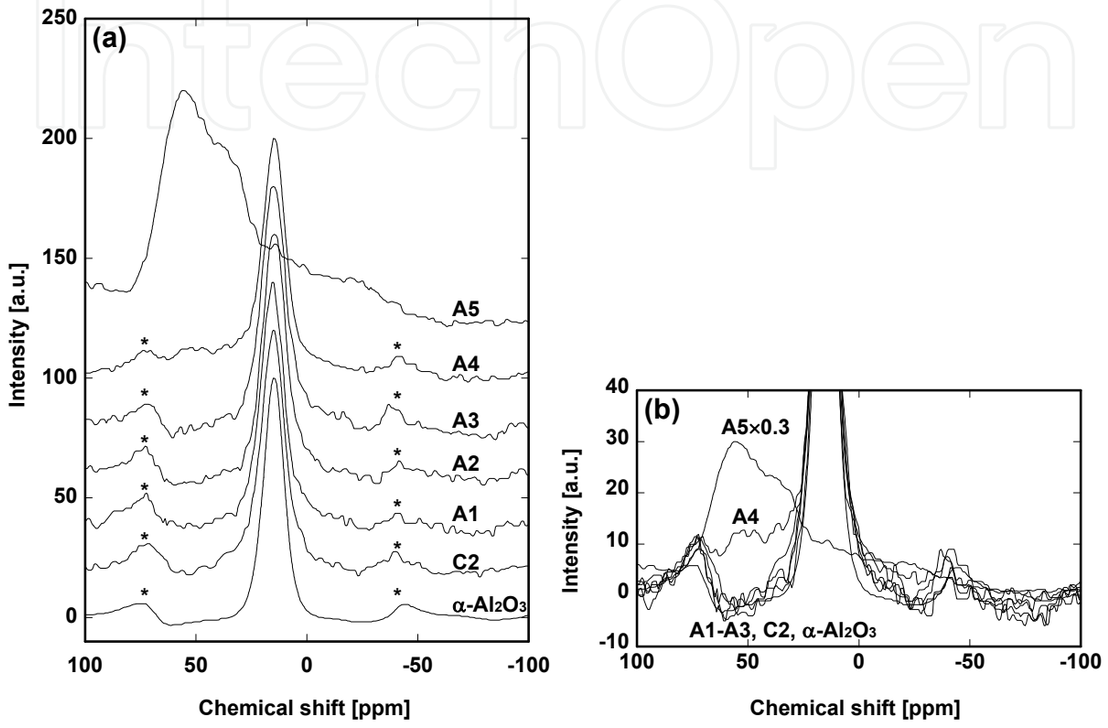

Fig. 6. ^{27}Al-NMR spectra of A1–A5, C2, and α-Al_2O_3: (a) whole view of spectra, and (b) expanded view of spectra in intensity scale

Sample A4, which includes Al_2O_3 of 2.3 mol%, has a weak 50 ppm peak in the ^{27}Al-NMR spectrum, while sample C2, which has the same amount of Al_2O_3 without Bi_2O_3, shows no signal around 50 ppm (Fig. 6(b)), suggesting that the Bi ion affects ACS over a 1.0 mol% of Bi_2O_3 concentration. On the other hand, since the C2 spectrum is dominated by a peak at 15 ppm, the aluminum ions in the silica glass naturally configure the 6-fold coordinated state of the corundum structure up to 2.3 mol% of Al_2O_3 without Bi_2O_3. This is also supported by the work of Mysen et al., who concluded the aluminum ions in silica glass work as a network modifier rather than a network former up to a 6.1 mol% Al_2O_3 concentration in the measurement of Raman spectra(Mysen, Virgo et al. 1980). The Al corundum structure dominates ACS at lower Bi concentration up to 0.5 mol%, so the Al corundum structure clearly has certain important roles for the generation of the Bi luminescent center in BiSG.

3.5 XRD measurements

The XRD data of the BiSG samples were measured to check for existing crystallizations, including undissolved alumina, mullite, or crystbalite because crystallization influences the ^{27}Al-NMR spectra. The measured samples are A-series. Fig. 7 shows the XRD data on

samples A4, α-Al_2O_3 (alumina), and pure silica with a range between 10 and 80° in 2θ. Sample A4 is substituted for the other BiSG ones because these XRD patterns are almost the same. The peaks due to any kind of crystallization are not recognized in Fig. 7, especially undissolved alumina, where there is only a halo pattern. We previously confirmed an XRD pattern on a Nd_2O_3(3 wt%; 0.55 mol%)-SiO_2(97 wt%; 99.45 mol%) system that included undissolved 0.55 mol% of Nd_2O_3 at best(Fujimoto & Nakatsuka 1997). 7.0 mol% of alumina (at maximum in this experiment) is probably an adequate quantity for XRD detection if the quantity is changed to undissolved alumina or other crystals in the sample. Therefore, it is concluded that all our samples are in the amorphous phase.

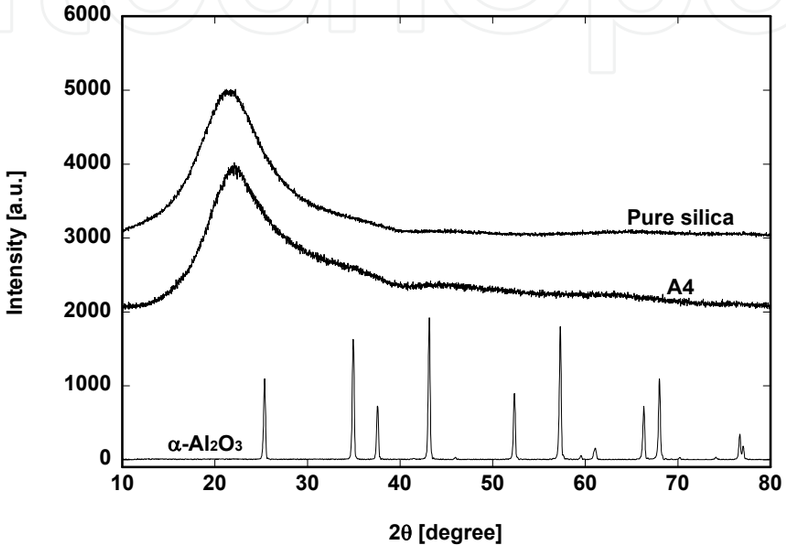

Fig. 7. XRD patterns on α-Al_2O_3 (alumina), sample A4 and pure silica with range between 10° and 80° in 2θ

3.6 ESR measurements

The presence of unpaired electrons in BiSG was verified by ESR signal. The measured sample was B2 and B3. There was no ESR signal due to the unpaired electrons for both B2 and B3, even at liquid N_2 temperature. The same phenomena without signals were also reported on Bi-doped multi-component glasses(Peng, Wang et al. 2005; Peng, Wu et al. 2008). According to Hund's rule, the valence states of bismuth ions without unpaired electrons should be Bi^{3+}(~$5d^{10}6s^2$) or Bi^{5+} (~$5d^{10}$)(Ohkura, Fujimoto et al. 2007).

3.7 XPS measurements

3.7.1 Analysis on chemical shift

The results of the XPS measurements are shown in Fig. 8. The measured samples were A4, A5, and three standards, $NaBiO_3$, Bi_2O_3, and Bi-metal. The main Bi($4f_{5/2}$, $4f_{7/2}$) peaks of Bi_2O_3 exist at 163.7 and 158.4 eV, respectively. Bi-metal was treated with 3-minute etching by Ar-beam in a vacuum chamber (1.0×10^{-7} Torr) to eliminate the oxidized Bi-metal surface before the measurement. Even after the treatment, weak residual peaks were found due to Bi_2O_3. The main Bi($4f_{5/2}$, $4f_{7/2}$) peaks of the Bi-metal exist at 162.4 and 157.1 eV, respectively. These Bi_2O_3 and Bi-metal peaks well agree with those previously reported(Wagner 1990; Saffarini

& Saiter 2000), and the chemical shifts of Bi_2O_3 and Bi-metal are very stable in the XPS measurement. $NaBiO_3$ is often used as a standard of the penta-valent state of Bi, but in our experiment, the main Bi($4f_{5/2}$, $4f_{7/2}$) peaks of $NaBiO_3$ were obtained at 163.8 and 158.5 eV corresponding to the Bi_2O_3 ones, and the second Bi($4f_{5/2}$, $4f_{7/2}$) peaks exist at higher bonding energy at 165.9 and 160.6 eV, respectively. The peaks of both BiSGs, that is, A4 and A5, are located at almost the same position at the second $NaBiO_3$ peaks. After arranging the chemical shifts for the measured samples, the order of the bonding energy is as follows:

[lower bonding energy] Bi metal (Bi^0) -> Bi_2O_3 (Bi^{3+}), first peaks of $NaBiO_3$ (Bi^{3+}) -> second peaks of $NaBiO_3$ (Bi^{5+}) = BiSG (A4, A5) [higher bonding energy]

In general, the valence state of the target ion becomes higher with increased bonding energy(Wagner 1990), and the same tendency is observed in my measurement. Therefore, Bi ions of the penta-valent state exist in BiSG.

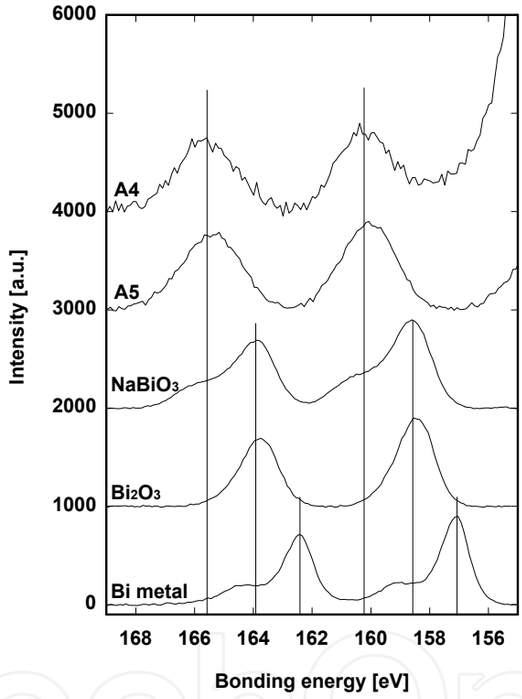

Fig. 8. XPS peaks of Bi($4f_{5/2}$, $4f_{7/2}$) on A4, A5, $NaBiO_3$, Bi_2O_3, and Bi-metal. In observation order of binding energy, [lower bonding energy] Bi metal (Bi^0) -> Bi_2O_3 (Bi^{3+}), first peaks of $NaBiO_3$ (Bi^{3+}) -> second peaks of $NaBiO_3$ (Bi^{5+}) = BiSG (A4, A5) [higher bonding energy].

The peak positions of $NaBiO_3$, however, seem unstable. The previously reported Bi($4f_{5/2}$, $4f_{7/2}$) peaks(Kulkarni, Vijayakrishnan et al. 1990) were 164.1 and 158.7 eV, respectively, and they showed single peaks with almost the same binding energy of the Bi_2O_3 ones. In fact, although we measured the XPS data on the $NaBiO_3$ several times, the ratio of the main peaks corresponding to Bi_2O_3 to the second peaks was unstable. Therefore, we put the most probable XPS data of $NaBiO_3$ in Fig. 8.

Kumada et al.(Kumada, Takahashi et al. 1996; Kumada, Kinomura et al. 1999) reported that $NaBiO_3$ and $LiBiO_3$ are synthesized at 120-200°C and that the Bi^{5+} state is changed to a Bi^{3+} state over 400°C; similar unstability may occur for the Bi^{5+} state in $NaBiO_3$. The standard

material of $NaBiO_3$ was identified as $NaBiO_3 \bullet 2H_2O$ by XRD in Kumada's experiment. They also reported that Na ions in the A-site ($A^+B^{5+}O_3$) tend to be exchanged for Sr^{2+} or Ba^{2+} ions in $NaBiO_3 \bullet nH_2O$, and then the redistributed Bi ions in the A-site take the Bi^{3+} state(Kumada, Kinomura et al. 1999). Although they neglected to mention the redistribution of Bi ions in $NaBiO_3$ themselves, a similar phenomenon may occur for $NaBiO_3$ in their experiment.

3.7.2 Analysis on peak separation

By precisely observing the peak positions and the line widths, we recognized that the A4 peaks were slightly shifted to higher bonding energy than A5 and that the line widths of A4 and A5 were wider than the standards. Since the A4 and A5 peaks are composed of two or more peaks, we separated them with a Gaussian fitting curve to examine the origin of the peak shift. In this procedure, we make the following assumptions:

1. If such Bi ionic states as Bi^0 or Bi^{3+} are considered identical, the line widths of Bi($4f_{5/2}$, $4f_{7/2}$) are also identical.
2. The line widths of Bi $4f_{5/2}$ and Bi $4f_{7/2}$ are the same.
3. The ratio of Bi $4f_{5/2}$ to Bi $4f_{7/2}$ is constant for different ionic states in a sample. This ratio is theoretically calculated as $Bi^4f_{5/2}/Bi^4f_{7/2}=l/(l+1)=3/4$(Seah 1983).

The results are shown in Table 3. The peak separation results show five peak positions for all Bi $4f_{5/2}$ and Bi $4f_{7/2}$ peaks that are normalized at 100. No. 5 corresponds to Bi^0, No. 4 to Bi^{3+}, and No. 1 to Bi^{5+}. Nos. 2 and 3 are the intermediate states between numbers 1 and 4, and these states have intermediate coordination states rather than intermediate valence states such as Bi^{4+} due to the ESR measurements. These results show that all the Bi ions in BiSG are not the penta-valent state, and therefore the Bi valence states were mixed states of Bi^{3+} with Bi^{5+}. This mixed valence state of Bi^{3+} and Bi^{5+} is also supported by EXAFS analysis

Sample		Bi $4f_{5/2}$(Bi $4f_{7/2}$)				
		1	2	3	4	5
A4	Peak [eV]	166.0(160.6)	164.9(159.5)			
	FWHM [eV]	1.7	1.7			
	Height	100.0	64.6			
A5	Peak [eV]	166.2(160.8)	165.1(159.8)			
	FWHM [eV]	1.9	1.9			
	Height	50.6	100.0			
$NaBiO_3$	Peak [eV]	165.9(160.6)		164.6(159.3)	163.8(158.5)	
	FWHM [eV]	1.8		1.4	1.4	
	Height	38.6		35.0	100.0	
α-Bi_2O_3	Peak [eV]			164.7(159.4)	163.7(158.4)	
	FWHM [eV]			1.4	1.4	
	Height			19.9	100.0	
Bi metal	Peak [eV]			164.6(159.3)	163.4(158.1)	162.4(157.1)
	FWHM [eV]			1.4	1.4	1.1
	Height			22.4	22.4	100.0

Table 3. Peak separation results on Bi($4f_{5/2}$, $4f_{7/2}$) of A4, A5, $NaBiO_3$, α-Bi_2O_3, and Bi-metal. Peak position, FWHM, and normalized peak height are listed. Peak-heights are normalized at 100.

in the next section. The peak height ratio of Nos. 1 and 2 is counterchanged for A4 and A5 due to the existence ratio of Bi^{3+} and Bi^{5+}. Thus, the peaks of A4 are slightly shifted due to higher bonding energy than A5.

3.8 Bi-O distance from EXAFS

Figure 9 shows the radial structure functions (RSF) to which the EXAFS oscillations were Fourier-transformed. The measured samples were A-series (A2~A5) and the two standards of α-Bi_2O_3 and $NaBiO_3$. The peak shown in about 1.0 Å is derived from the XANES region because it is too short for any Bi-O distance. Therefore, it is a ghost peak, and we conclude that the largest peak around 1.6-1.7 Å (the first relevant peak) corresponds to the first neighboring Bi-O bond. α-Bi_2O_3 and $NaBiO_3$ have the second peak at 3.5 and 3.2 Å, respectively. Since the BiSG ones have no secondary peak, the local environment of the Bi ion does not have any periodical structure; that is, BiSG should be an amorphous phase. These results are supported by the XRD data in Section 3.5. The RSF shows that all the BiSG peaks are about 0.1 Å shorter than α-Bi_2O_3. The $NaBiO_3$ peak is also shifted to a shorter position, but the line width is wider than that of any of the BiSG ones. Since RSF $|F(r)|$ includes a phase shift, the radial distance in RSF shifted a shorter range than the actual Bi-O distance. To determine the length of the first neighboring Bi-O, the RSF of α-Bi_2O_3 and the BiSG samples were analyzed by the curve-fitting method in r-space with *FEFF 8.2*. In this curve-fitting calculation, we only took two coordination spheres due to the parameter number limitation in *FEFF 8.2*.

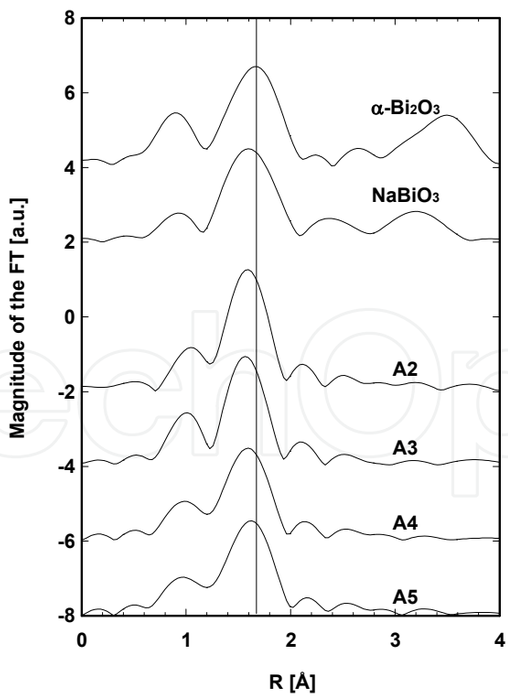

Fig. 9. Radial structure functions (RSF) of A-series (A2~A5), α-Bi_2O_3 and $NaBiO_3$

The fitting results of the BiSG samples, α-Bi_2O_3 and $NaBiO_3$, are listed in Table 4. We assumed amplitude reduction factor S_0^2 = 0.9(Manzini, Lottici et al. 1998) and absorption

edge energy E_0 = 13426.5 eV. The fitting range was selected from 1.2 to 2.1 Å in RSF (Fig. 9). The Bi-O distances of the first and second coordination spheres for BiSG were calculated as about 2.1 and 2.3 Å, respectively; on the other hand, the Bi-O distances for α-Bi_2O_3 were 2.2 and 2.4 Å, respectively. The Bi-O distance of 2.1 Å in BiSG is in good agreement with the previously reported Bi^{5+}-O distance in $LiBi(5+)O_3$(Kumada, Takahashi et al. 1996) and $Bi_2(3+,5+)O_4$(Kumada, Kinomura et al. 1995). Therefore, the existence of the Bi^{5+} state is also indicated from the Bi-O distance in BiSG, and the first coordination sphere corresponds to the Bi^{5+}-O distance. The second coordination sphere of 2.3Å corresponds to the Bi^{3+}-O distance(Ohkura, Fujimoto et al. 2007). Therefore, the EXAFS curve-fitting results also show that the mixed valence state of the Bi ions exists in BiSG as Bi^{3+} and Bi^{5+}.

The Bi-O distance of the first coordination sphere in the A-series is slightly shifted to a longer range with increased Bi_2O_3 concentration in Table 4. The ratio of Bi^{3+} to Bi^{5+} increases with increased Bi_2O_3 concentration, and the change of the Bi^{3+} to Bi^{5+} ratio can also explain the non-linear increment of LMI. $NaBiO_3$ is a well-known material as a standard for penta-valent state Bi ions. The first coordination state distance of $NaBiO_3$ is longer than the expected value of the Bi^{5+}-O distance. This valence state of Bi ions in $NaBiO_3$ is also the mixed state of Bi^{3+} and Bi^{5+}. These phenomena are also supported by the peak separation data of XPS.

Samples	First coordination sphere			Second coordination sphere			R-factor(%)
	N_1	R_1	σ_1^2(Å^2)	N_2	R_2	σ_2^2(Å^2)	
α-Bi_2O_3	2.01	2.18	3.91E-03	0.74	2.40	4.07E-03	8.82
$NaBiO_3$	7.15	2.13	3.89E-03	3.12	2.38	4.06E-03	0.89
A2	2.19	2.08	3.89E-03	1.11	2.32	4.06E-03	1.65
A3	2.05	2.08	3.89E-03	1.33	2.31	4.06E-03	2.50
A4	1.81	2.11	3.89E-03	1.05	2.31	4.06E-03	2.84
A5	1.86	2.13	3.89E-03	0.99	2.33	4.06E-03	3.04

Table 4. FEFF fitting results providing two coordination spheres. Fitting results of A-series (A2~A5), α-Bi_2O_3, and $NaBiO_3$ are listed.

3.9 Discussion (local structure of luminescent center)

In the previous section, several physical phenomena were observed in BiSG, especially regarding the local structure of the distinctive luminescent center. Now we consider the structural configuration on the Bi luminescent center.

First, the roles of the Al_2O_3 additive can be understood by luminescent intensity measurement. Based on Fig. 5, the luminescent intensity of A4, which includes 2.3 mol% of Al_2O_3, is three orders of magnitude larger than that of C1 without Al_2O_3; clearly, the Al_2O_3 additive remarkably increases the generation of the Bi luminescent center. Second, Al_2O_3 assists the Bi ions to enter the silica glass network because C1 has no glassy wetting. This tendency is also supported by the phase diagram of the Bi_2O_3-Al_2O_3-SiO_2 glass system, because the glassy phase is likely achieved at the Al_2O_3-rich composition. Therefore, aluminum ions have two roles in BiSG:

1. They assist the configuration of the distinctive luminescent center of Bi ions with a coupling effect that denotes that an aluminum ion behaves like a "generator" of the luminescent center.
2. They increase compatibility with the silica network.

These aluminum ion roles imply that both the Bi and Al atoms should be close together in BiSG. Based on the above discussion, the image view between Bi and Al ions in BiSG is illustrated in Fig. 10(a). Peng et al.(Peng, Qiu et al. 2005) reported that Ta ions also work as a "generator." Although aluminum is not the only element that behaves as a generator, the aluminum ion accepts its important role in the Bi_2O_3-Al_2O_3-SiO_2 glass system.

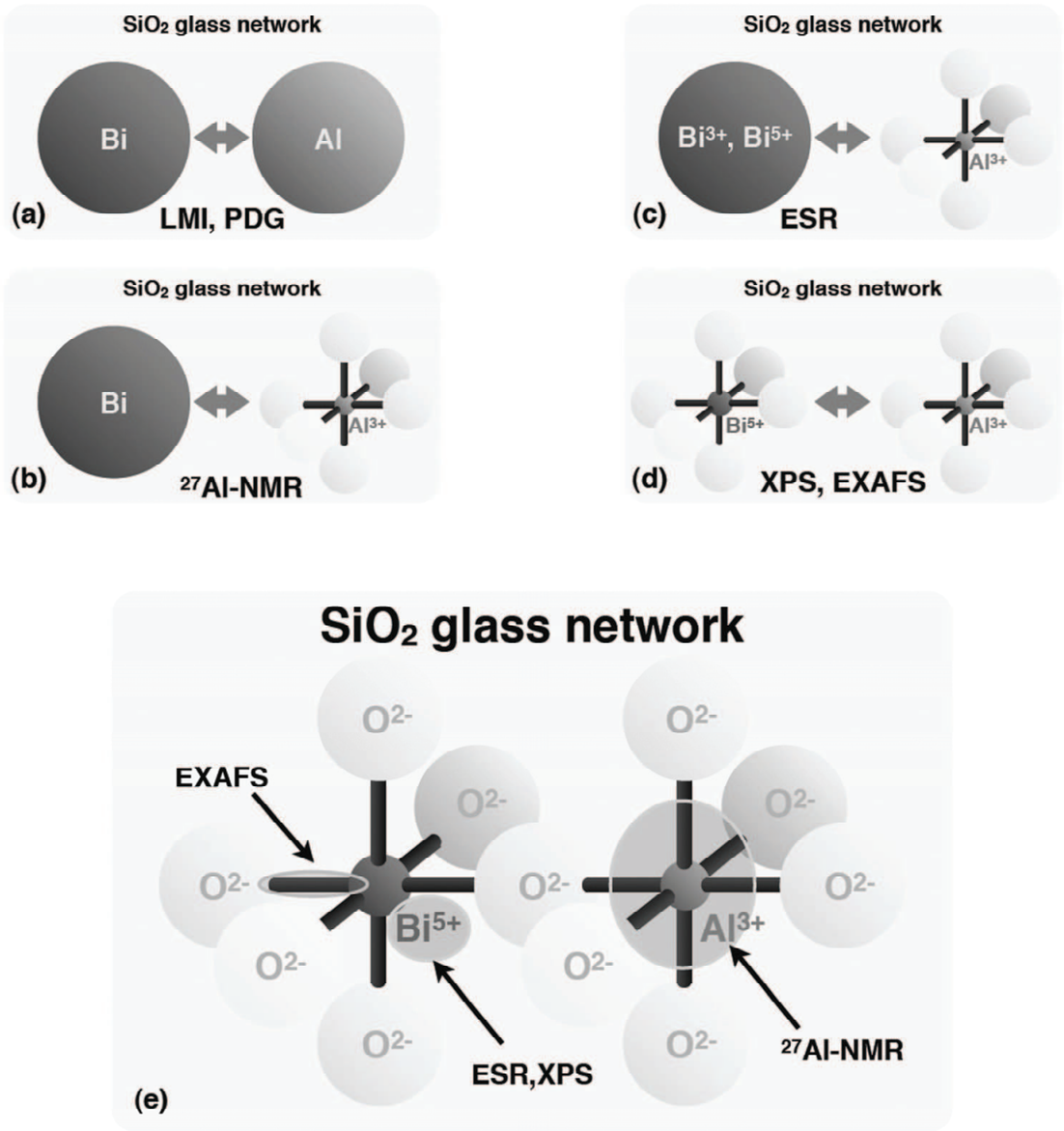

Fig. 10. Image view on local structure of infrared Bi luminescent center in BiSG: (a) image view determined by PDG (phase diagram) and LMI, (b) by ^{27}Al-NMR, (c) by ESR, (d) by XPS, EXAFS, (e) local structure of infrared Bi luminescent center.

Next, the aluminum cordination state (ACS) should be close to the Bi ion in BiSG, as seen from the ^{27}Al-NMR results. Since the relation between ACS and the chemical shift in the ^{27}Al-NMR measurement has been well studied(Laussac, Enjalbert et al. 1983), ACS is determined by a chemical shift in comparison between the standard materials and the target samples. In the case of BiSG, ACS is dominated by the α-Al_2O_3 corundum structure at lower Bi_2O_3 concentration up to 0.5 mol%. Al ions with corundum structure are crucial to generate a distinctive luminescent center, and the Al coordination state located near Bi should be a 6-fold corundum structure. Based on the above discussion, the image view between Bi and Al is illustrated in Fig. 10(b).

Next, information on the valence states of the Bi ions in BiSG is given by ESR measurements. Of course, it's not only for Bi ions, but since no signal exists for the unpaired electrons in the whole BiSG, the valence states of Bi ions without unpaired electrons are Bi^{3+} or Bi^{5+}. These results show Bi^{3+} or Bi^{5+} ions close to the 6-fold coordination state of the Al ions. Based on the above discussion, the image view between Bi and Al is illustrated in Fig. 10(c).

Three types of coordination states of Bi^{3+} exist, including 5-, 6-, and 8-fold; on the other hand, only 6-fold coordination exists for Bi^{5+}(Shannon 1976). Since BiSG is an oxide material, it is estimated that the neighboring ions of the Bi ion are oxygen. Although the ionic radius of O^{2-} has few differences with the coordination number, variation exists between 1.35 and 1.42 Å. If the coordination number of O^{2-} is 4, Bi^{3+}(5)-O^{2-}(4), Bi^{3+}(6)-O^{2-}(4), and Bi^{5+}(6)-O^{2-}(4) are calculated to be 2.34, 2.41, and 2.12 Å, respectively(Shannon 1976). The Bi-O distances in typical crystals including Bi^{3+} or Bi^{5+}, such as $LiBiO_3$(Kumada, Takahashi et al. 1996) or Bi_2O_4(Kumada, Kinomura et al. 1995), show that the Bi^{5+}-O distance is 2.1 Å. This value agrees well with the 2.1 Å of the first coordination sphere for A4 and A5. But the Bi^{3+}-O distance varies from 2.15 to 3.26 Å in α-Bi_2O_3(Harwig 1978) or Bi_2O_4(Kumada, Kinomura et al. 1995). Therefore, the EXAFS data show that the Bi^{5+} ionic state exists in BiSG, and this is also supported by the XPS data. The previously reported Bi^{3+} spectroscopic properties are quite different in luminescent and absorption spectra and lifetime. It is concluded that the Bi valence state of the Bi luminescent center is Bi^{5+}, not Bi^{3+}. Therefore, the luminescent center model of Bi^{5+} with 6-fold coordination is expected to be close to Al^{3+} with 6-fold coordination of the corundum structure (Fig. 10(d)). Since the neighboring atom is oxygen, the local structure of the distinctive bismuth luminescent center is expected (Fig. 10(e)).

4. Applications

After the discovery of a new infrared luminescent bismuth center, several research groups started to study its applications, such as optical amplification(Fujimoto & Nakatsuka 2003; Seo, Fujimoto et al. 2006; Seo, Fujimoto et al. 2006; Ren, Wu et al. 2007; Ren, Dong et al. 2007; Ren, Qiao et al. 2007; Seo, Lim et al. 2007), waveguide inscription(Psaila, Thomson et al. 2006), or laser oscillation(Dianov, Dvoyrin et al. 2005; Dianov, Shubin et al. 2007; Razdobreev, Bigot et al. 2007; Rulkov, Ferin et al. 2007; Truong, Bigot et al. 2008) using Bi luminescent materials.

With respects to device applications, optical fibers with Bi luminescent center in the core material are very curious. Optical amplification around 1.3 μm with Bi-doped multi-component glass fiber was achieved by Seo et al.(Seo, Fujimoto et al. 2006), and this is useful for metro area network optical amplifiers. Laser oscillation with Bi-doped optical fiber was firstly demonstrated by Dianov's group in 2005(Dianov, Dvoyrin et al. 2005), then the possibility of Bi-doped fiber is actively developed, now the oscillation power has achieved

at 15 W at 1160 nm(Bufetov & Dianov 2009). It is known that the 570 – 590 nm band is very promising for ophthalmology and dermatology applications, thus the second harmonic of Bi fiber laser can be used in medical use. And the broad luminescence in near infrared region is also useful for a light source of optical coherence tomography.

5. Conclusions

In this chapter, we introduce the basic properties of BiSG and the analyzed local structure of Bi luminescent center. Several instrumental analyses, such as spectroscopic properties (SPCT), LMI, NMR, XRD, ESR, XPS, and EXAFS were advanced on a Bi_2O_3-Al_2O_3-SiO_2 glass system. The roles and the structure of the Al ions and the valence state of the luminescent Bi ions were examined.

The following are the roles and the structure of the Al ions: 1) to assist the configuration of the distinctive luminescent center of Bi ions with a coupling effect, which means that the aluminum ion behaves like a "generator" of the luminescent center; 2) to increase compatibility with the silica network; 3) to be a 6-fold corundum structure. The valence state exmination of Bi ions in BiSG reveals the following: 1) Bi^{3+} or Bi^{5+}; 2) a mixed state of Bi^{3+} and Bi^{5+}; 3) Bi^{5+} for the distinctive Bi luminescent center. Therefore, the distinctive bismuth luminescent center model was investigated with a 6-fold coordination state of Bi^{5+} that is combined with the 6-fold corundum structure of Al^{3+} through an oxygen ion (Fig. 10(e)). These results will bridge to verify the energy diagram and the mechanism of Bi luminescent center.

In the last place, this new infrared luminescent material, Bi-doped silica glass, which attains sensational progress in the past decade will continue to give us curious possibilities in the field of the optical science.

6. Acknowledgement

The EXAFS measurement in this work was performed under the approval of the Photon Factory Program Advisory Committee (Proposal No. 2006G123).

7. References

M. J. Weber and R. R. Monchamp (1973). Luminescence of Bi4Ge3O12 : Spectral and decay properties. *J. Appl. Phys.*, Vol.44, 5495-5499.

S. Parke and R. S. Webb (1973). Optical Properties of Thallium, Lead and Bismuth in Oxide Glasses. *Journal of Physics and Chemistry of Solids*, Vol.34, No.1, 85-95.

R. D. Shannon (1976). Revised Effective Ionic-Radii and Systematic Studies of Interatomic Distances in Halides and Chalcogenides. *Acta Crystallographica Section A*, Vol.32, No.Sep1, 751-767.

H. A. Harwig (1978). Structure of Bismuthsesquioxide - Alpha,Beta,Gamma and Delta-Phase. *Zeitschrift Fur Anorganische Und Allgemeine Chemie*, Vol.444, No.Sep, 151-166.

B. O. Mysen, D. Virgo, et al. (1980). Relations between the Anionic Structure and Viscosity of Silicate Melts - a Raman-Spectroscopic Study. *American Mineralogist*, Vol.65, No.7-8, 690-710.

A. C. van der Steen, J. J. A. van Hesteren, et al. (1981). Luminescence of the Bi-3+ Ion in Compounds LiLnO2 and NaLnO2 (Ln=Sc, Y, La, Gd, Lu). *Journal of the Electrochemical Society*, Vol.128, No.6, 1327-1333.

D. B. a. M. P. Seah (1983). Practical surface analysis : by auger and X-ray photo-electron spectroscopy. New York, Wiley.

J. P. Laussac, R. Enjalbert, et al. (1983). Tetracoordinated, Penta-Coordinated and Hexacoordinated Aluminum - Nmr and X-Ray-Diffraction Studies of the Complexes of Ethylenediamine with Aluminum Isopropoxide and Its Fluoro Analogs. *Journal of Coordination Chemistry*, Vol.12, No.3, 133-143.

C. D. Wagner (1990). Auger and x-ray photoelectron spectroscopy. New York, John Wiley.

G. U. Kulkarni, V. Vijayakrishnan, et al. (1990). State of Bismuth in BaBiO3 and BaBi1-xPbxO3 - Bi 4f Photoemission and Bi L3 Absorption Spectroscopic Studies. *Applied Physics Letters*, Vol.57, No.17, 1823-1824.

H. Scholze (1991). Glass : nature, structure, and properties. New York, Springer-Verlag.

S. N. Narang, N. D. Patel, et al. (1994). Infrared and Raman Spectral Studies and Normal-Modes of Alpha-Bi2O3. *Journal of Molecular Structure*, Vol.327, No.2-3, 221-235.

N. Kumada, N. Kinomura, et al. (1995). Crystal-Structure of Bi2O4 with Beta-Sb2O4-Type Structure. *Journal of Solid State Chemistry*, Vol.116, No.2, 281-285.

N. Sugimoto, H. Kanbara, et al. (1996). Ultrafast response of third-order optical nonlinearity in glasses containing Bi2O3. *Optics Letters*, Vol.21, No.20, 1637-1639.

N. Kumada, N. Takahashi, et al. (1996). Preparation and crystal structure of a new lithium bismuth oxide: LiBiO3. *Journal of Solid State Chemistry*, Vol.126, No.1, 121-126.

Y. Fujimoto and M. Nakatsuka (1997). A novel method for uniform dispersion of the rare earth ions in SiO2 glass using zeolite X. *Journal of Non-Crystalline Solids*, Vol.215, No.2-3, 182-191.

I. Manzini, P. P. Lottici, et al. (1998). EXAFS at the BiLIII edge in Bi4Ge3O12 and in xBi(2)O(3)-(100-x)GeO2 glasses. *Journal of Non-Crystalline Solids*, Vol.224, No.1, 23-30.

N. Kumada, N. Kinomura, et al. (1999). Ion-exchange reaction of Na+ in NaBiO3 center dot nH(2)O with Sr2+ and Ba2+. *Solid State Ionics*, Vol.122, No.1-4, 183-189.

PDF#30-1161 (2000). Powder diffraction file : alphabetical indexes for experimental patterns : inorganic phases : sets 1-50. Newtown Square, Pa. , ICDD, International Center for Diffraction Data.

G. Saffarini and J. M. Saiter (2000). X-ray photoelectron spectroscopic measurements on glassy Ge20S80-xBix (x=0,16). *Materials Letters*, Vol.46, No.6, 327-331.

Y. Fujimoto and M. Nakatsuka (2001). Infrared luminescence from bismuth-doped silica glass. *Japanese Journal of Applied Physics Part 2-Letters*, Vol.40, No.3B, L279-L281.

Y. Fujimoto and M. Nakatsuka (2003). Optical amplification in bismuth-doped silica glass. *Applied Physics Letters*, Vol.82, No.19, 3325-3326.

M. Y. Peng, J. R. Qiu, et al. (2004). Bismuth- and aluminum-codoped germanium oxide glasses for super-broadband optical amplification. *Optics Letters*, Vol.29, No.17, 1998-2000.

M. Y. Peng, X. G. Meng, et al. (2005). GeO2 : Bi, M (M = Ga, B) Glasses with Super-Wide Infrared Luminescence. *Chemical Physics Letters*, Vol.403, No.4-6, 410-414.

M. Y. Peng, J. R. Qiu, et al. (2005). Broadband infrared luminescence from Li2O-Al2O3-ZnO-SiO2 glasses doped with Bi2O3. *Optics Express*, Vol.13, No.18, 6892-6898.

M. Y. Peng, J. R. Qiu, et al. (2005). Superbroadband 1310 nm emission from bismuth and tantalum codoped germanium oxide glasses. *Optics Letters*, Vol.30, No.18, 2433-2435.

E. M. Dianov, V. V. Dvoyrin, et al. (2005). CW bismuth fibre laser. *Quantum Electronics*, Vol.35, No.12, 1083-1084.

X. G. Meng, J. R. Qiu, et al. (2005). Infrared broadband emission of bismuth-doped barium-aluminum-borate glasses. *Optics Express*, Vol.13, No.5, 1635-1642.

X. G. Meng, J. R. Qiu, et al. (2005). Near infrared broadband emission of bismuth-doped aluminophosphate glass. *Optics Express*, Vol.13, No.5, 1628-1634.

M. Y. Peng, C. Wang, et al. (2005). Investigations on bismuth and aluminum co-doped germanium oxide glasses for ultra-broadband optical amplification. *Journal of Non-Crystalline Solids*, Vol.351, No.30-32, 2388-2393.

Y. Fujimoto and M. Nakatsuka (2006). Al-27 NMR structural study on aluminum coordination state in bismuth doped silica glass. *Journal of Non-Crystalline Solids*, Vol.352, No.21-22, 2254-2258.

Y. S. Seo, Y. Fujimoto, et al. (2006). Optical amplification in a bismuth-doped silica glass at 1300 nm telecommunications window. *Optics Communications*, Vol.266, No.1, 169-171.

Y. S. Seo, Y. Fujimoto, et al. (2006). Simultaneous amplification at two wavelengths near 1300 nm in a 6.5-cm-long bismuth-doped silica glass. *Ieee Photonics Technology Letters*, Vol.18, No.17-20, 1901-1903.

X. J. Wang and H. P. Xia (2006). Infrared superbroadband emission of Bi ion doped germanium-aluminum-sodium glass. *Optics Communications*, Vol.268, No.1, 75-78.

T. Suzuki and Y. Ohishi (2006). Ultrabroadband near-infrared emission from Bi-doped Li2O-Al2O3-SiO2 glass. *Applied Physics Letters*, Vol.88, No.19, 191912.

H. P. Xia and X. J. Wang (2006). Near infrared broadband emission from Bi5+-doped Al2O3-GeO2-X (X=Na2O,BaO,Y2O3) glasses. *Applied Physics Letters*, Vol.89, No.5, 051917.

N. D. Psaila, R. R. Thomson, et al. (2006). Femtosecond laser inscription of optical waveguides in bismuth ion doped glass. *Optics Express*, Vol.14, No.22, 10452-10459.

V. V. Dvoyrin, V. M. Mashinsky, et al. (2006). Bismuth-doped-glass optical fibers - a new active medium for lasers and amplifiers. *Optics Letters*, Vol.31, No.20, 2966-2968.

T J. J. Ren, L. Y. Yang, et al. (2006). Effect of various alkaline-earth metal oxides on the broadband infrared luminescence from bismuth-doped silicate glasses. *Solid State Communications*, Vol.140, No.1, 38-41.

T. Ohkura, Y. Fujimoto, et al. (2007). Local structures of bismuth ion in bismuth-doped silica glasses analyzed using bi L-III x-ray absorption fine structure. *Journal of the American Ceramic Society*, Vol.90, No.11, 3596-3600.

Y. Fujimoto, Y. Hirata, et al. (2007). Effect of GeO2 additive on fluorescence intensity enhancement in bismuth-doped silica glass. *Journal of Materials Research*, Vol.22, No.3, 565-568.

E. M. Dianov, A. V. Shubin, et al. (2007). High-power cw bismuth-fiber lasers. *Journal of the Optical Society of America B-Optical Physics*, Vol.24, No.8, 1749-1755.

T. Murata and T. Mouri (2007). Matrix effect on absorption and infrared fluorescence properties of Bi ions in oxide glasses. *Journal of Non-Crystalline Solids*, Vol.353, No.24-25, 2403-2407.

M. Y. Peng, D. P. Chen, et al. (2007). Bismuth-doped zinc aluminosilicate glasses and glass-ceramics with ultra-broadband infrared luminescence. *Optical Materials*, Vol.29, No.5, 556-561.

I. Razdobreev, L. Bigot, et al. (2007). Efficient all-fiber bismuth-doped laser. *Applied Physics Letters*, Vol.90, No.3, -.

J. Ren, B. Wu, et al. (2007). Broadband optical amplification near 1300 nm in bismuth-doped germanate glass. *Applied Physics B-Lasers and Optics*, Vol.88, No.3, 363-366.

J. J. Ren, H. F. Dong, et al. (2007). Ultrabroadband infrared luminescence and optical amplification in bismuth-doped germanosilicate glass. *Ieee Photonics Technology Letters*, Vol.19, No.17-20, 1395-1397.

J. J. Ren, Y. B. Qiao, et al. (2007). Optical amplification near 1300 nm in bismuth-doped strontium germanate glass. *Journal of the Optical Society of America B-Optical Physics*, Vol.24, No.10, 2597-2600.

J. J. Ren, J. R. Qiu, et al. (2007). Infrared luminescence properties of bismuth-doped barium silicate glasses. *Journal of Materials Research*, Vol.22, No.7, 1954-1958.

J. J. Ren, J. R. Qiu, et al. (2007). Ultrabroad infrared luminescence from Bi-doped aluminogermanate glasses. *Solid State Communications*, Vol.141, No.10, 559-562.

J. J. Ren, J. R. Qiu, et al. (2007). Ultrabroad infrared luminescences from Bi-doped alkaline earth metal germanate glasses. *Journal of Materials Research*, Vol.22, No.6, 1574-1578.

A. B. Rulkov, A. A. Ferin, et al. (2007). Narrow-line, 1178nm CW bismuth-doped fiber laser with 6.4W output for direct frequency doubling. *Optics Express*, Vol.15, No.9, 5473-5476.

Y. S. Seo, C. Lim, et al. (2007). Bismuth-doped silica glass as a new laser material. *Journal of the Korean Physical Society*, Vol.51, No.1, 364-367.

G. Yang, D. P. Chen, et al. (2007). Effects of melting temperature on the broadband infrared luminescence of bi-doped and Bi/Dy co-doped chalcohalide glasses. *Journal of the American Ceramic Society*, Vol.90, No.11, 3670-3672.

S. F. Zhou, G. F. Feng, et al. (2007). Broadband near-infrared emission from Bi-doped aluminosilicate glasses. *Journal of Materials Research*, Vol.22, No.6, 1435-1438.

Y. Arai, T. Suzuki, et al. (2007). Ultrabroadband near-infrared emission from a colorless bismuth-doped glass. *Applied Physics Letters*, Vol.90**,** No.26, 261110.

V. G. Truong, L. Bigot, et al. (2008). Study of thermal stability and luminescence quenching properties of bismuth-doped silicate glasses for fiber laser applications. *Applied Physics Letters*, Vol.92, No.4, 041908.

J. J. Ren, G. P. Dong, et al. (2008). Inhomogeneous broadening, luminescence origin and optical amplification in bismuth-doped glass. *Journal of Physical Chemistry A*, Vol.112, No.14, 3036-3039.

J. R. Qiu, M. Y. Peng, et al. (2008). Novel Bi-doped glasses for broadband optical amplification. *Journal of Non-Crystalline Solids*, Vol.354, No.12-13, 1235-1239.

M. Y. Peng, B. T. Wu, et al. (2008). Bismuth-activated luminescent materials for broadband optical amplifier in WDM system. *Journal of Non-Crystalline Solids*, Vol.354, No.12-13, 1221-1225.

I. A. Bufetov and E. M. Dianov (2009). Bi-doped fiber lasers. *Laser Physics Letters*, Vol.6, No.7, 487-504.

Advances in Solid State Lasers Development and Applications

Edited by Mikhail Grishin

ISBN 978-953-7619-80-0
Hard cover, 630 pages
Publisher InTech
Published online 01, February, 2010
Published in print edition February, 2010

Invention of the solid-state laser has initiated the beginning of the laser era. Performance of solid-state lasers improved amazingly during five decades. Nowadays, solid-state lasers remain one of the most rapidly developing branches of laser science and become an increasingly important tool for modern technology. This book represents a selection of chapters exhibiting various investigation directions in the field of solid-state lasers and the cutting edge of related applications. The materials are contributed by leading researchers and each chapter represents a comprehensive study reflecting advances in modern laser physics. Considered topics are intended to meet the needs of both specialists in laser system design and those who use laser techniques in fundamental science and applied research. This book is the result of efforts of experts from different countries. I would like to acknowledge the authors for their contribution to the book. I also wish to acknowledge Vedran Kordic for indispensable technical assistance in the book preparation and publishing.

How to reference

In order to correctly reference this scholarly work, feel free to copy and paste the following:

Yasushi Fujimoto (2010). New Infrared Luminescence from Bi-doped Glasses, Advances in Solid State Lasers Development and Applications, Mikhail Grishin (Ed.), ISBN: 978-953-7619-80-0, InTech, Available from: http://www.intechopen.com/books/advances-in-solid-state-lasers-development-and-applications/new-infrared-luminescence-from-bi-doped-glasses

INTECH
open science | open minds

InTech Europe
University Campus STeP Ri
Slavka Krautzeka 83/A
51000 Rijeka, Croatia
Phone: +385 (51) 770 447
Fax: +385 (51) 686 166
www.intechopen.com

InTech China
Unit 405, Office Block, Hotel Equatorial Shanghai
No.65, Yan An Road (West), Shanghai, 200040, China
中国上海市延安西路65号上海国际贵都大饭店办公楼405单元
Phone: +86-21-62489820
Fax: +86-21-62489821

© 2010 The Author(s). Licensee IntechOpen. This chapter is distributed under the terms of the Creative Commons Attribution-NonCommercial-ShareAlike-3.0 License, which permits use, distribution and reproduction for non-commercial purposes, provided the original is properly cited and derivative works building on this content are distributed under the same license.

IntechOpen

IntechOpen